Time-like electromagnetic form factors of Λ, Σ, and Ξ^+ in a light-front quark model

Chong-Chung Lih[*] and Chao-Qiang Geng[†]
Chongqing University of Posts and Telecommunications, Chongqing 400065, China
and School of Fundamental Physics and Mathematical Sciences, Hangzhou Institute for Advanced Study, UCAS, Hangzhou 310024, China

(Received 8 January 2026; revised 21 March 2026; accepted 10 April 2026; published 12 May 2026)

We use the light front quark model to investigate the form factors in the $e^+e^- \to B\bar{B}$ collision proceses with $B = \Lambda,\ \Sigma$ and Ξ. These form factor behaviors are calculated based on the Bethe-Salpeter formalism with $q^+ > 0$ to effectively account for nonvalence contributions. We show that our results of the q^2-dependent form factors closely match the BESIII data. In particular, we obtain that $|G_{\rm eff}| = (0.921,\ 0.098,\ 0.189)$ and $R = |\frac{G_E}{G_M}| = (0.97,\ 0.89,\ 0.936)$ for $e^+e^- \to \Lambda\bar{\Lambda},\ \Sigma^+\Sigma^-,\ \Xi^+\Xi^+)$ with $q^2 = (5.74,\ 6.0,\ 7.0)\,\text{GeV}^2$.

DOI: 10.1103/nsvk-4sjg

I. INTRODUCTION

Understanding the internal structure of hadrons has always been a great challenge. Quantum chromodynamics (QCD) uses quarks and gluons (i.e., QCD degrees of freedom) to describe the structure of hadrons and their interactions. We are accustomed to believe that the motion of quarks and gluons inside hadrons will change under the action of strong fields in nuclear matter, and such changes are expected to be reflected in the electromagnetic and weak structures of nucleons and other baryons [1–3]. A commonly used parametrization for the electromagnetic structure of hadrons is the electromagnetic form factor (EMFF), which is an observable quantity of non-perturbative QCD and is also a key to understand bound-state QCD effects. Therefore, the EMFF can be used to explore the internal structure of baryons and experimentally detected through the interaction of hadrons with virtual photons.

Another possibility for revealing the electromagnetic structure of baryons is the e^+e^- scattering. It allows us to enter the time-like regime ($q^2 = -Q^2 \geqslant 0$), which was proposed long ago by Cabibbo and Gatto [4]. The $e^+e^- \to B\bar{B}$ (and its inverse) reaction offers new opportunities for studying valence quark effects, diquark pairs (diquarks), and the role of different quark compositions [5–11]. This time-like form factor appears to be a viable tool for determining hyperon structures, both near the threshold and in the larger q^2 region, where perturbation effects are expected to be dominant [4,10–16]. In recent years, $e^+e^- \to B\bar{B}$ and $p^+p^- \to B\bar{B}$ experiments [10,17–21] have been able to detect the structure of short-lived baryons in the timelike kinematic region above the threshold $4M_B^2$ (where M_B is the baryon mass). The experiments at BaBar [22], BESIII [23,24], and CLEO [10,11] have also provided data related to the electromagnetic form factor of timelike hyperons. These timelike studies complement our understanding of the spacelike region ($q^2 \leqslant 0$) [25–27] based on electron scattering experiments over the past two decades.

The light front quark model (LFQM), a phenomenological model previously used extensively to study the form factors of meson weak decays, operates not only directly in the time-like regime but also in the space-like regime. Using the "+" component of the current in the Drell-Yan-West ($q^+ = q_0 + q_z = 0$) framework, the form factors of decays in the space-like regime ($q^2 < 0$) can be calculated, along with contributions from valence and Fock states. Another option is to use the same "+" component but in the $q^+ \neq 0$ regime, i.e., the timelike regime ($q^2 > 0$). Physically, particle decay processes occur in the time-like regime, so in principle, the form factors can be calculated in the $q^+ \neq 0$ framework in the time-like regime. However, operating in the time-like regime may yield contributions from nonvalence Fock states [28], requiring the wave function to have higher Fock states. This means that we will inevitably encounter nonvalence diagrams arising from the production of quark-antiquark pairs. As shown in Fig. 1(b) and (c), the collision process $e^+e^- \to B\bar{B}$ is a typical nonvalence diagram. Fortunately, the literature already provides effective methods for dealing with nonvalence contributions in meson-incompatible processes [28–31]. The goal of our method is to use this procedure to directly calculate the form factor in the $e^+e^- \to B\bar{B}$ collision process and compare it with the experimental data.

This paper is organized as follows. In Sec. II, we present the framework for the form factors of $e^+e^- \to B\bar{B}$. Our numerical results and discussions are given in Sec. III. We conclude in Sec. IV.

II. A FRAMEWORK FOR $e^+e^- \to B\bar{B}$

The reaction where a lepton pair l^+l^- into a $B\bar{B}$ pair, viz.

$$l^+l^- \to \gamma^* \to B\bar{B}, \tag{1}$$

[*]Contact author: cclih123@gmail.com
[†]Contact author: cqgeng@ucas.ac.cn

Published by the American Physical Society under the terms of the Creative Commons Attribution 4.0 International license. Further distribution of this work must maintain attribution to the author(s) and the published article's title, journal citation, and DOI. Funded by SCOAP³.

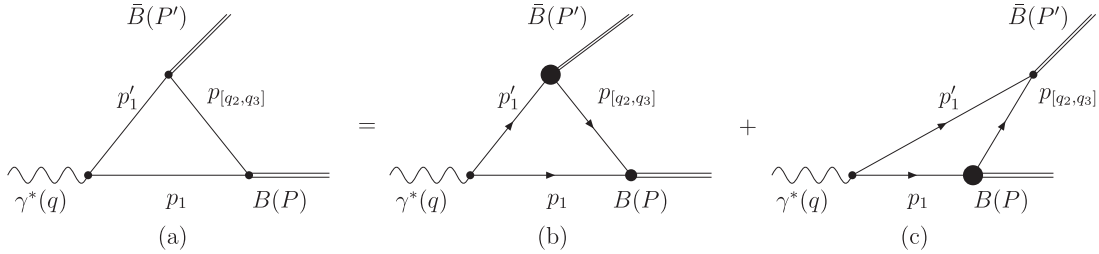


FIG. 1. The effective treatment of the LF amplitude (a) can be displayed into two parts in the regions of (b) $0 < x < 1$ and (c) in $1 < x < 1/\zeta$, where the small and big dots of the mediator-quark vertices in (b) and (c) represent the LF ordinary and nonvalence wavefunction vertices, respectively.

is a direct source of information on nuclear form factors in the time-like region. These is a one-photon-exchange for the electron-positron annihilation into a $B\bar{B}$ pair and is produced only for $q^2 \geqslant 4M_B^2$. In particular, to investigate the process of Eq. (1), the matrix elements of the nucleon current operator involved in this reaction are written as follows [32,33]:

$$\sqrt{\frac{EE'}{M_B^2}}(2\pi)^3\langle B(P,S)\bar{B}(P',S')|J^\mu_{em}(0)|0\rangle = \bar{u}_S(P)\left[\gamma^\mu f_1(q^2) + i\frac{f_2(q^2)}{2M_B}\sigma^{\mu\nu}q_\nu\right]v_{S'}(P'), \quad (2)$$

where $q^\mu = P^\mu + P'^\mu$ and $f_i (i = 1, 2)$ are the baryonic form factors. In the time-like region, the current operator participates in transitions from vacuum to a state containing hadron pairs, which becomes a real state beyond the intrinsic threshold given by $q^2 = 4M_B^2$.

Employing the single-photon approximation, the form shown in Eq. (2) is the most general possible form, but it is not the only concise expression. For the baryon pair production differential cross section, after transforming from the center-of-mass frame to the laboratory frame, we obtain [4,32,33]

$$\frac{d\sigma}{d\Omega}|_{(l^+l^-\to B\bar{B})} = \frac{\alpha^2\beta}{4q^2}\left\{(1+\cos^2\theta)\,|G_M(q^2)|^2 + \frac{\sin^2\theta}{\tau}\,|G_E(q^2)|^2\right\}, \quad (3)$$

where α is fine structure constant, $\beta = \sqrt{1-\frac{4M_B^2}{q^2}}$, $\tau = \frac{q^2}{4M_B^2}$, θ is the angle between the direction of the incoming electron and the produced hardron, $G_E(q^2)$ and $G_M(q^2)$ are the charge and magnetic form factor, respectively. In comparison to Eq. (2), one has

$$G_E = f_1(q^2) + \tau f_2(q^2),\ G_M = f_1(q^2) + f_2(q^2). \quad (4)$$

Compared to the traditional form factors $f_1(q^2)$ and $f_2(q^2)$, the simplified charge form factor $G_E(q^2)$ and magnetic form factor $G_M(q^2)$ provide greater clarity for discussing experimental data. Integrating the solid angle Ω over the expression Eq. (3), one obtains

$$\sigma_{(l^+l^-\to B\bar{B})} = \frac{4\pi\alpha^2\beta}{3q^2}\left\{|G_M(q^2)|^2 + \frac{|G_E(q^2)|^2}{2\tau}\right\}. \quad (5)$$

Therefore, an effective form factor can be defined as follows:

$$|G_{\rm eff}| = \sqrt{\frac{2\tau|G_M(q^2)|^2 + |G_E(q^2)|^2}{1+2\tau}}. \quad (6)$$

According to Eq. (2), to calculate the form factors, we employe a light-front quark model in the time-like region. In the LFQM, we treat baryons containing three quarks as bound states composed of a single quark q_1 and a diquark $q_{[2,3]}$, wherein the diquark $q_{[2,3]}$ comprises q_2 and q_3. Explicitly, the baryon bound state with the total momentum P and spin $S = \frac{1}{2}$ can be written as [34]

$$|B(P,S,S_z)\rangle = \int\{d^3p_1\}\{d^3p_{[q_2,q_3]}\}2(2\pi)^3\delta^3(\tilde{P}-\tilde{p}_1-\tilde{p}_{[q_2,q_3]}) \times \sum_{\lambda_1,\lambda_2}\Psi^{SS_z}(p_1, p_{[q_2,q_3]}, \lambda_1, \lambda_2)|q_1(p_1,\lambda_1) \times [q_2,q_3](p_{[q_2,q_3]},\lambda_2)\rangle, \quad (7)$$

where q_1 denotes the active quark of the baryon, $[q_2, q_3]$ represents the diquark, Ψ^{SS_z} corresponds to the momentum-space wave function, and $p_{1,2}$ are the on-mass-shell light front momenta

$$p = (p^+, p_\perp),\quad p_\perp = (p^1, p^2),\quad p^- = \frac{m^2+p_\perp^2}{p^+} \quad (8)$$

with

$$p_1^+ = x_1P^+,\quad p^+_{[q_2,q_3]} = x_2P^+,\quad x_1+x_2 = 1,$$
$$p_{1\perp} = x_1P_\perp + k_\perp,\quad p_{[q_2,q_3]\perp} = x_2P_\perp - k_\perp. \quad (9)$$

In Eq. (9), $(x, k_\perp)$ are the light-front relative momentum variables, and $\vec{k}_\perp$ is the component of the internal momentum $\vec{k} = (\vec{k}_\perp, k_z)$.

By the Melosh transformation [35], it is more convenient to work with the following representation of the wave function

$$\Psi^{SS_z}(p_1, p_{[q_2,q_3]}, \lambda_1, \lambda_2) = \frac{1}{\sqrt{2(p_1\cdot P + m_1M_0)}}\bar{u}(p_1,\lambda_1)\Gamma_{l,m}u(P,S_z)\phi(x,k_\perp), \quad (10)$$

where $\Gamma_{l,m}$ is the coupling vertex function of the decaying quark q_1 and the diquark in the baryon state. For the scalar diquark, the coupling vertex is $\Gamma_s = 1$. If the axial-vector

diquark is involved, the vertex should be

$$\Gamma_A = -\frac{1}{\sqrt{3}}\gamma_5 \not{\epsilon}^*(p_{[q_2,q_3]}, \lambda_2). \tag{11}$$

The wave function of $\phi(x, k_\perp)$ in Eq. (10) describes the momentum distribution of the constituent quarks in the bound state. In this work, we use the Gaussian-type function, given as

$$\phi(x, k_\perp) = 4\left(\frac{\pi}{\beta^2}\right)^{3/4}\sqrt{\frac{dk_z}{dx}}\exp\left(\frac{-\vec{k}^2}{2\beta^2}\right), \tag{12}$$

where β is the baryon shape parameter and k_z is defined by

$$k_z = \frac{xM_0}{2} - \frac{m_2^2 + k_\perp^2}{2xM_0}, \quad M_0 = e_1 + e_2 \tag{13}$$

and

$$M_0^2 = \frac{m_1^2 + k_\perp^2}{1-x} + \frac{m_2^2 + k_\perp^2}{x}, \tag{14}$$

where $e_i = \sqrt{m_i^2 + \vec{k}^2}$ and $\vec{k} = (k_\perp, k_z)$. In our calculation, we assume

$$\zeta \equiv \frac{P^+}{q^+} = \frac{q^2 + M_B^2 - M_{\bar{B}}^2 - \sqrt{(q^2 + M_B^2 - M_{\bar{B}}^2)^2 - 4M_B^2 q^2}}{2q^2}. \tag{15}$$

Using the bound states of $|B(P, S, S_z)\rangle$ and $|\bar{B}(P', S', S'_z)\rangle$ in Eq. (7) and the above identities, we derive the matrix elements of the baryonic transition in the LF frame. By considering the $\mu = +$ component, the transition matrix elements are given by

$$\langle B(P, S, S_z)\bar{B}(P', S', S'_z)|\bar{q}\gamma^+ q|0\rangle = N_{fs}\int \{d^4p_2\}\frac{\Lambda_B(x, \mathbf{k}_\perp) I^+ \Lambda'_{\bar{B}}(x', \mathbf{k'}_\perp)}{(p_1^2 - m_1^2 + i\epsilon)(p_1'^2 - m_1'^2 + i\epsilon)}, \tag{16}$$

where $I^+ = \sum_{\lambda_2}\bar{u}(P, S_z)[\bar{\Gamma}'_{S(A)}(\not{p}'_1 + m'_1)\gamma^+(\not{p}_1 + m_1)\Gamma_{S(A)}] \times v(P', S'_z)$, $\Lambda_B(\Lambda'_{\bar{B}})$ corresponds to the vertex function of the baryon $B(\bar{B})$, $\bar{\Gamma} = \gamma^0\Gamma^\dagger\gamma^0$ and N_{fs} is a flavor-spin factor given in Ref. [36]. The trace term I^+ in Eq. (16) can be written as the sum of I_1^+ and I_2^+, as shown in Fig. 1. In the region of $0 < p_1^+ < P^+$ and $p_1^- = p_{1on}^- = (m_1^2 + k_\perp^2)/p_1^+$, the baryon $\bar{B}$ will possess a nonvalence vertex, as seen in Fig. 1(b). The effective contribution of the LF amplitude is given by [37–40]

$$\mathcal{M} = \frac{N_{fs}}{16\pi^3}\int_0^1 dx \int d^2\mathbf{k}_\perp \frac{\Gamma_g(x, \mathbf{k}_\perp) I_1^+}{(1-x)(x'-1)P^+P'^+}\Psi_B(x, \mathbf{k}_\perp) \times \int \frac{dy}{y(1-y)}\int d^2\mathbf{l}_\perp \mathcal{K}_{\bar{B}}(x, \mathbf{k}_\perp; y, \mathbf{l}_\perp)\Psi'_{\bar{B}}(y, \mathbf{l}_\perp),$$
$$I_1^+ = \bar{u}(P, S_z)\bar{\Gamma}'(\not{p}'_1 + m'_1)\gamma^+(\not{p}_1 + m_1)\Gamma v(P', S'_z). \tag{17}$$

The wave function corresponding to the nonvalence vertex is usually obtainable from the Bethe-Salpeter (BS) amplitude in the BS theory [28,41]. The LF BS equation is expressed as [28,42,43]

$$\left(M^2 - M_0^2\right)\Psi'_{\bar{B}}(x_i, k_{i\perp}) = \int [dy][d^2\mathbf{l}_\perp]\mathcal{K}(x_i, k_{i\perp}; y_j, \mathbf{l}_{j\perp})\Psi'_{\bar{B}}(y_j, \mathbf{l}_{j\perp}). \tag{18}$$

The nonvalence BS amplitudes can be regarded as solutions of Eq. (18). For the baryon, the normal and nonvalence BS amplitudes correspond to $x < 1$ and $x > 1$, respectively. We note that Eq. (18) essentially takes the same form as the LF bound-state equation except the difference in kinematics. In Fig. 1(b), the nonvalence BS amplitude is the analytic continuation of the valence BS amplitude. In the LFQM, the relationship between the BS amplitudes of two regions is given in Refs. [28–30]. However, for the integral equation of Eq. (18) it is necessary to use the nonperturbative QCD method to obtain the kernel. Following Refs. [37–40], we obtain the transition form factors

$$f_1(q^2) = \frac{N_{fs}}{16\pi^3}\int_0^1 dx \int d^2\mathbf{k}_\perp \frac{\Gamma_g(x, \mathbf{k}_\perp) I_{f_1}^+}{(1-x)(x'-1)P^+P'^+}\Psi_B(x, \mathbf{k}_\perp) \times \int \frac{dy}{y(1-y)}\int d^2\mathbf{l}_\perp \mathcal{K}_{\bar{B}}(x, \mathbf{k}_\perp; y, \mathbf{l}_\perp)\Psi'_{\bar{B}}(y, \mathbf{l}_\perp),$$
$$I_{f_1}^+ = \mathrm{Tr}[(\not{P}' + M')\gamma^+(\not{P} + M)(\not{p}'_1 + m'_1)\gamma^+(\not{p}_1 + m_1)],$$
$$\frac{f_2(q^2)}{2M_B} = \frac{N_{fs}}{16\pi^3}\int_0^1 dx \int d^2\mathbf{k}_\perp \frac{\Gamma_g(x, \mathbf{k}_\perp) I_{f_2}^+}{(1-x)(x'-1)P^+P'^+q_\perp^\nu}\Psi_B(x, \mathbf{k}_\perp)\int \frac{dy}{y(1-y)}\int d^2\mathbf{l}_\perp \mathcal{K}_{\bar{B}}(x, \mathbf{k}_\perp; y, \mathbf{l}_\perp)\Psi'_{\bar{B}}(y, \mathbf{l}_\perp),$$
$$I_{f_2}^+ = \mathrm{Tr}[(\not{P}' + M')\sigma^{\nu+}(\not{P} + M)(\not{p}'_1 + m'_1)\gamma^+(\not{p}_1 + m_1)], \tag{19}$$

where $\nu = 1, 2$ and the trace term in Eq. (19) should be separated into the on-shell propagating and instantaneous parts of $I_{\rm on}^\mu$ and $I_{\rm inst}^\mu$ via

$$\not{p}' + m = (\not{p}'_{\rm on} + m) + \tfrac{1}{2}\gamma^+(p^- - p_{\rm on}^-), \tag{20}$$

respectively. Both $I_{\rm on}^\mu$ and $I_{\rm inst}^\mu$ are components of the trace term, originating from the first and second terms on the right-hand side of Eq. (20), respectively. The explicit forms of the above form factors can be expressed as functions of the internal variables of x and $k_\perp$. In Eq. (19), Γ_g is a vertex function for the gauge boson associated with the LF energy denominator with its explicit form given by [28,30,44]

$$\Gamma_g^{-1}(x, \mathbf{k}_\perp) = (1-\zeta)\left[q_\perp^2 - \left(\frac{\mathbf{k}_\perp^2 + m_1^2}{\zeta(1-x)} + \frac{\mathbf{k}'^2_\perp + m_1'^2}{1-\zeta-\zeta x}\right)\right]. \tag{21}$$

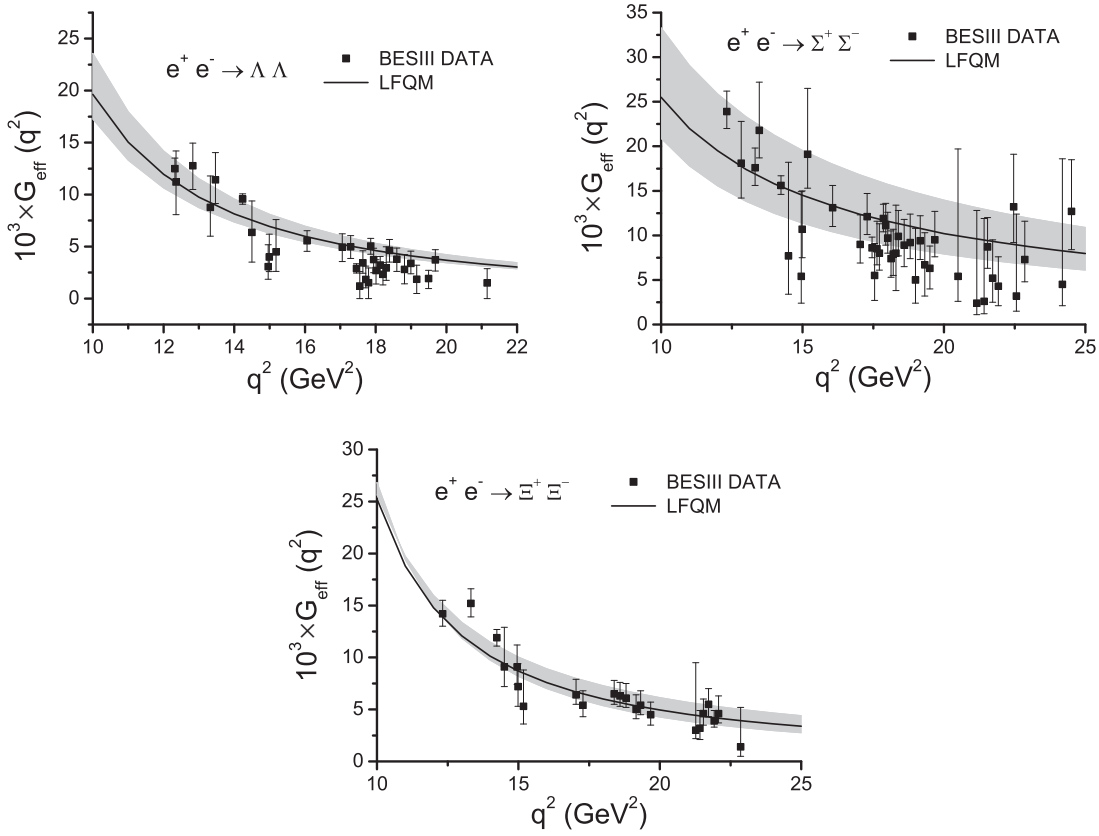


FIG. 2. Form factors of $e^+e^- \to B\bar{B}$.

The trace terms in Eqs. (17) and (19), both corresponding to the products of the initial and final LF spin wave functions, can be obtained by off-shell Melosh transformations. The form factors related to Fig. 1(b) are given by

$$f_1(q^2) = \frac{N_{fs}}{16\pi^3}\int_0^1 dx \int d^2\mathbf{k}_\perp \Gamma_g(x,\mathbf{k}_\perp)\Psi_B(x,\mathbf{k}_\perp) \times \frac{[k_\perp\cdot k'_\perp + ((1-x_1)M_0+m_1)((1-x'_1)M'+m'_1)] + I^+_{\rm inst}}{(1-x)(x'-1)}$$
$$\times \int \frac{dy}{y(1-y)} \int d^2\mathbf{l}_\perp \mathcal{K}_{\bar{B}}(x,\mathbf{k}_\perp;y,\mathbf{l}_\perp)\Psi'_{\bar{B}}(y,\mathbf{l}_\perp),$$
$$\frac{f_2(q^2)}{2M_B} = \frac{N_{fs}}{16\pi^3}\int_0^1 dx \int d^2\mathbf{k}_\perp \Gamma_g(x,\mathbf{k}_\perp)\Psi_B(x,\mathbf{k}_\perp) \times \frac{[(m_1+(1-x_1)M_0)k'_\perp\cdot q_\perp - (m'_1+(1-x'_1)M')k_\perp\cdot q_\perp] + I'^+_{\rm inst}}{(1-x)(x'-1)q^2_\perp}$$
$$\times \int \frac{dy}{y(1-y)} \int d^2\mathbf{l}_\perp \mathcal{K}_{\bar{B}}(x,\mathbf{k}_\perp;y,\mathbf{l}_\perp)\Psi'_{\bar{B}}(y,\mathbf{l}_\perp), \tag{22}$$

where the instantaneous component $I^{(\prime)+}_{\rm inst}$ of the nonvalence diagram in Eq. (22) is zero during this process.

The relevant operator $\mathcal{K}(\mathcal{K}_{\bar{B}})$ in Eqs. (18), (19), and (22) is the BS core, which in principle contains contributions from high Fock states. It is the high Fock component of the bound state related to the lowest Fock component with this kernel. The kernel functions can be obtained by using the nonperturbative QCD. The kernel $\mathcal{K}$ is a function of all internal momenta $(x,\mathbf{k}_\perp,y,\mathbf{l}_\perp)$. We define that $G_{B\bar{B}} \equiv \int [dy][d^2\mathbf{l}_\perp]\mathcal{K}_{\bar{B}}(x,\mathbf{k}_\perp;y,\mathbf{l}_\perp)\Psi_{\bar{B}}(y,\mathbf{l}_\perp)$, which depends only on x and $\mathbf{k}_\perp$. The range of the momentum fraction x relies on the external momenta for the embedded states.

In the region of $1 < x < 1/\zeta$, $P^+ < p_1^+ < q^+$, and $p'^-_1 = p'^-_{1on} = (m'^2_1 + k'^2_{1\perp})/p'^+_1$. At this point, the vertex of the baryon B enters the nonvalence region, while the vertex of baryon $\bar{B}$ the valence region, as shown in Fig. 1(c). For the transition form factors, we may directly exchange the following parameters in Eq. (19):

$$x \leftrightarrow x',\ m_1 \leftrightarrow m'_1,\ p_1 \leftrightarrow p'_1,\ \Psi_B \leftrightarrow \Psi'_{\bar{B}}. \tag{23}$$

III. NUMERICAL RESULTS AND DISCUSSIONS

We present numerical results on the form factors of the $e^+e^- \to B\bar{B}$ transitions in the time-like region for the LFQM.

TABLE I. Form factors of the $e^+e^- \to B\bar{B}$ transition.

$e^+e^- \to \Lambda\Lambda$	$F(q^2 = 5.7408\ \text{GeV}^2)$	a	b
G_E	$0.456^{+0.112}_{-0.074}$	-193.38	1391.17
G_M	$0.462^{+0.113}_{-0.078}$	-157.969	1133.79
$e^+e^- \to \Sigma^+\Sigma^-$	$F(q^2 = 6.0\ \text{GeV}^2)$	a	b
G_E	$0.0451^{+0.0041}_{-0.0003}$	-14.716	91.45
G_M	$0.0512^{+0.0036}_{-0.0002}$	-13.478	83.93
$e^+e^- \to \Xi^+\Xi^-$	$F(q^2 = 7.0\,\text{GeV}^2)$	a	b
G_E	$0.0903^{+0.0237}_{-0.0156}$	-74.80	384.711
G_M	$0.0965^{+0.0245}_{-0.0164}$	-53.141	273.371

Computationally, we hope to find a time-domain-like result, so we only introduce $q_\perp = 0$ in the final numerical calculation. In our calculations, we use [34]

$$m_{u,d} = 0.25,\ m_s = 0.38,\ m_{[qq']} = 0.7,\ \beta_{s[qq]} = 0.4 \pm 0.05,$$
$$\beta_{u[qq]} = 0.2 \pm 0.1. \tag{24}$$

In Eq. (22), $G_{B\bar{B}}$ is taken as a constant in the range of 0.1–6.0, which was previously tested in some exclusive semileptonic decay processes and shown to be a good approximation for processes with a small momentum transfer [28,30]. Explicitly, we choose $G_{B\bar{B}} = 1.8$, 1.0, and 0.3 for $\Lambda\Lambda$, $\Sigma^+\Sigma^+$, and $\Xi^+\Xi^+$, respectively, in our numerical evaluation.

To describe the momentum q^2 behaviors, we parametrize the form factors in the double-pole forms of

$$F(q^2) = \frac{F(0)}{1 + a(q^2/m_P^2) + b(q^4/m_P^4)} \tag{25}$$

with $m_P = 6.0$ GeV for all modes of $e^+e^- \to B\bar{B}$ in M_B mass scalar, and $[F(0), a, b]$ to be determined in the numerical analysis. Our results for the form factors are given in Table I. In our results, the errors come from uncertainties in the parameters of β.

In Fig. 2, we present our evaluations of the form factors as functions of q^2 for the $e^+e^- \to \Lambda\Lambda$, $\Sigma^+\Sigma^-$, and $\Xi^+\Xi^-$ transitions, respectively, where the BESIII data fits are also given. From the figures, we compare the LF model calculations for $|G_{\text{eff}}|$ with the BESIII data of $\Lambda\Lambda$, $\Sigma^+\Sigma^-$, and $\Xi^+\Xi^-$ for $q^2 \geqslant 10\,\text{GeV}^2$. This comparison shows that the LF model describes the data well above $q^2 \geqslant 10\,\text{GeV}^2$ within the theoretical limit. Current calculations for $|G_{\text{eff}}|$ indicate that the region $q^2 \geqslant 10\,\text{GeV}^2$ is within the range, where the asymptotic behavior of the form factor can be observed. However, it is important to note that the current data may still be in the nonperturbative QCD regime. Figure 2 shows that the form factors exhibit a similar behaviors throughout the q^2 spectra. Obviously, our LFQM results with the non-valence contributions are consistent with the BESIII data [45–47]. We also use this model to calculate the $|G_E/G_M|$ ratios for the processes $e^+e^- \to (\Lambda\bar{\Lambda},\ \Sigma^+\Sigma^-,\ \Xi^+\Xi^-)$. For the three processes mentioned above, at $q^2 = (5.7408, 6.0, 7.0)\,\text{GeV}^2$, we get $|G_{\text{eff}}| = (0.921^{+0.22}_{-0.15},\ 0.098^{+0.002}_{-0.0002},\ 0.189^{+0.048}_{-0.032})$, and $R = |\frac{G_E}{G_M}| = (0.985 \pm 0.001,\ 0.88 \pm 0.01,\ 0.936 \pm 0.004)$.

IV. CONCLUSION

The e^+e^- collision experiments explore the electromagnetic properties of elementary particles. Under the electromagnetic interaction at the tree level, e^+e^- annihilation processes can occur via virtual photons with timelike four-momenta, which subsequently decay into final states. In this work, we have used the LFQM to investigate the form factors in the $e^+e^- \to B\bar{B}$ collision process. In particular, we have analyzed the form factors for the baryon transition based on the BS formalism with $q^+ > 0$, effectively accounting for nonvalence contributions. We have found that the q^2 behaviors of the form factors are consistent with the BESIII data. As shown in Table II, for the processes $e^+e^- \to (\Lambda\bar{\Lambda}, \Sigma^+\Sigma^-,\ \Xi^+\Xi^+)$ at $q^2 = (5.74,\ 6.0,\ 7.0)\,\text{GeV}^2$, our results are $|G_{\text{eff}}| = (0.921, 0.098, 0.189)$ and $R = |G_E/G_M| = (0.97, 0.89, 0.936)$, the results including nonvalence contributions agree with existing BESIII experimental data and other theoretical estimates.

ACKNOWLEDGMENTS

This work is supported in part by the National Natural Science Foundation of China (NSFC) under Grant No. 12547104.

DATA AVAILABILITY

The data that support the findings of this article are openly available [45–47].

[1] G. E. Brown and M. Rho, Scaling effective Lagrangians in a dense medium, Phys. Rev. Lett. **66**, 2720 (1991).
[2] W. K. Brooks, S. Strauch, and K. Tsushima, Medium modifications of hadron properties and partonic processes, J. Phys.: Conf. Ser. **299**, 012011 (2011).
[3] K. Saito, K. Tsushima, and A. W. Thomas, Nucleon and hadron structure changes in the nuclear medium and impact on observables, Prog. Part. Nucl. Phys. **58**, 1 (2007).
[4] N. Cabibbo and R. Gatto, Electron-positron colliding beam experiments, Phys. Rev. **124**, 1577 (1961).

[5] P. Kroll, T. Pilsner, M. Schürmann, and W. Schweiger, On exclusive reactions in the time-like region, Phys. Lett. B **316**, 546 (1993).

[6] R. Jakob, P. Kroll, M. Schürmann, and W. Schweiger, Octet-baryon form factors in the diquark model, Z. Phys. A **347**, 109 (1993).

[7] R. L. Jaffeand and F. Wilczek, Diquarks and exotic spectroscopy, Phys. Rev. Lett. **91**, 232003 (2003).

[8] F. Wilczek, Diquarks as inspiration and as objects, in *From Fields to Strings: Circumnavigating Theoretical Physics*, edited by Shifman Misha *et al.* (World Scientific, 2005), pp. 77–93.

[9] A. Selem and F. Wilczek, Hadron systematics and emergent diquarks, in *New Trends in HERA Physics 2005* (World Scientific, 2006), pp. 337–356.

[10] S. Dobbs, K. K. Seth, A. Tomaradze, T. Xiao, and G. Bonvicini, Hyperon form factors and diquark correlations, Phys. Rev. D **96**, 092004 (2017).

[11] S. Dobbs, A. Tomaradze, T. Xiao, K. K. Seth, and G. Bonvicini, First measurements of timelike form factors of the hyperons, Λ^0, Σ^0, Σ^+, Ξ^0, Ξ^-, and Ω^-, and evidence of diquark correlations, Phys. Lett. B **739**, 90 (2014).

[12] S. Pacetti, R. Baldini Ferroli, and E. Tomasi-Gustafsson, Proton electromagnetic form factors: Basic notions, present achievements and future perspectives, Phys. Rep. **550-551**, 1 (2015).

[13] B. Aubert *et al.* (BABAR Collaboration), Study of $e^+e^- \to p\bar{p}$ using initial state radiation with *BABAR*, Phys. Rev. D **73**, 012005 (2006).

[14] K. K. Seth, S. Dobbs, Z. Metreveli, A. Tomaradze, T. Xiao, and G. Bonvicini, Electromagnetic structure of the proton, pion, and kaon by high-precision form factor measurements at large timelike momentum transfers, Phys. Rev. Lett. **110**, 022002 (2013).

[15] K. Schonning and C. Li, Future perspectives on baryon form factor measurements with BES III, EPJ Web Conf. **137**, 12002 (2017).

[16] C. Li (BESIII Collaboration), Measurements of baryon form factors at BESIII, J. Phys.: Conf. Ser. **742**, 012020 (2016).

[17] M. Ablikim *et al.* (BESIII Collaboration), Measurement of the proton form factor by studying $e^+e^- \to p\bar{p}$, Phys. Rev. D **91**, 112004 (2015).

[18] M. Ablikim *et al.* (BESIII Collaboration), Future physics programme of BESIII, Chin. Phys. C **44**, 040001 (2020).

[19] M. Ablikim *et al.* (BESIII Collaboration), Complete measurement of the Λ electromagnetic form factors, Phys. Rev. Lett. **123**, 122003 (2019).

[20] M. Ablikim *et al.* (BESIII Collaboration), Determination of the Σ^+ timelike electromagnetic form factors, Phys. Rev. Lett. **132**, 081904 (2024).

[21] G. Ramalho, M. T. Pena, and K. Tsushima, Hyperon electromagnetic timelike elastic form factors at large q^2, Phys. Rev. D **101**, 014014 (2020).

[22] B. Aubert *et al.* (BABAR Collaboration), Study of $e^+e^- \to \Lambda\bar{\Lambda}$, $\Lambda\bar{\Sigma}^0$, $\Sigma^0\bar{\Sigma}^0$ using initial state radiation with *BABAR*, Phys. Rev. D **76**, 092006 (2007).

[23] M. Ablikim *et al.* (BESIII Collaboration), Search for baryonic decays of $\psi(3770)$ and $\psi(4040)$, Phys. Rev. D **87**, 112011 (2013).

[24] M. Ablikim *et al.* (BESIII Collaboration), Observation of a cross-section enhancement near mass threshold in $e^+e^- \to \Lambda\bar{\Lambda}$, Phys. Rev. D **97**, 032013 (2018).

[25] I. G. Aznauryan, A. Bashir, V. Braun, S. J. Brodsky, V. D. Burkert, L. Chang, C. Chen, B. El-Bennich, I. C. Cloet, P. L. Cole *et al.*, Studies of nucleon resonance structure in exclusive meson electroproduction, Int. J. Mod. Phys. E **22**, 1330015 (2013).

[26] I. G. Aznauryan and V. D. Burkert, Electroexcitation of nucleon resonances, Prog. Part. Nucl. Phys. **67**, 1 (2012).

[27] G. Ramalho and M. T. Pena, Electromagnetic transition form factors of baryon resonances, Prog. Part. Nucl. Phys. **136**, 104097 (2024).

[28] S. J. Brodsky and D. S. Hwang, Exact light-cone wavefunction representation of matrix elements of electroweak currents, Nucl. Phys. B **543**, 239 (1999); C. R. Ji and H. M. Choi, New effective treatment of the light-front nonvalence contribution in timelike exclusive processes, Phys. Lett. B **513**, 330 (2001).

[29] C. R. Ji and H. M. Choi, New progress in time-like exclusive processes, arXiv:hep-ph/0105248v3; Invited talk presented at the "2001 e^+e^- Physics at intermediate energies workshop", Stanford, CA, April 30–May 2, 2001, eConf C010430:T23, arXiv:hep-ph/0105248.

[30] H. M. Choi, C. R. Ji, and L. S. Kisslinger, Skewed quark distribution of the pion in the light-front quark model, Phys. Rev. D **64**, 093006 (2001).

[31] C.-C. Lih and C.-Q. Geng, Semileptonic decays of Λ_c^+ in light-front quark model with nonvalence contributions, Phys. Rev. D **112**, 076023 (2025).

[32] A. Denig and G. Salme, Nucleon electromagnetic form factors in the timelike region, Prog. Part. Nucl. Phys. **68**, 113 (2013).

[33] A. Zichichi, S. M. Berman, N. Cabibbo, and R. Gatto, Proton-antiproton annihilation into electrons, muons and vector bosons, IL Nuovo Cimento **24**, 170 (1962).

[34] H. G. Dosch, M. Jamin, and B. Stech, Diquarks, QCD sum rules, and weak decays, Z. Phys. C **42**, 167 (1989).

[35] H. J. Melosh, Quarks: Currents and constituents, Phys. Rev. D **9**, 1095 (1974).

[36] Z. X. Zhao, Weak decays of heavy baryons in the light-front approach, Chin. Phys. C **42**, 093101 (2018).

[37] S. Tawfiq, P. J. O'Donnell, and J. G. Korner, Charmed baryon strong coupling constants in a light-front quark model, Phys. Rev. D **58**, 054010 (1998).

[38] H.-C. Pauli, A compendium of light-cone quantization, Nucl. Phys. Proc. Suppl. **90**, 259 (2000).

[39] G. P. Lepage and S. J. Brodsky, Exclusive processes in perturbative quantum chromodynamics, Phys. Rev. D **22**, 2157 (1980).

[40] F. Schlumpf, Relativistic constituent quark model of electroweak properties of baryons, Phys. Rev. D **47**, 4114 (1993); **49**, 6246(E) (1994).

[41] B. L. G. Bakker and C.-R. Ji, Disentangling intertwined embedded states and spin effects in light-front quantization, Phys. Rev. D **62**, 074014 (2000); B. L. G. Bakker, H.-M. Choi, and C.-R. Ji, Regularizing the divergent structure of light-front currents, *ibid.* **63**, 074014 (2001).

[42] S. J. Brodsky, C.-R. Ji, and M. Sawicki, Evolution equation and relativistic bound-state wave functions for scalar-field models in four and six dimensions, Phys. Rev. D **32**, 1530 (1985).

[43] J. H. O. Sales, T. Frederico, B. V. Carlson, and P. U. Sauer, Light-front Bethe-Salpeter equation, Phys. Rev. C **61**, 044003 (2000).

[44] H. M. Choi, C. R. Ji, and L. S. Kisslinger, Light-front quark model analysis of rare $B \to Kl^+l^-$ decays, Phys. Rev. D **65**, 074032 (2002).

[45] M. Ablikim *et al.* (BESIII Collaboration), Measurement of the cross section for $e^+e^- \to \Lambda\bar{\Lambda}$ and evidence of the decay $\psi(3770) \to \Lambda\bar{\Lambda}$, Phys. Rev. D **104**, L091104 (2021); Measurement of the $e^+e^- \to \Lambda\bar{\Lambda}$ cross section from threshold to 3.00 GeV using events with initial-state radiation, **107**, 072005 (2023).

[46] M. Ablikim *et al.* (BESIII Collaboration), Measurement of Born cross section of $e^+e^- \to \Sigma^+\bar{\Sigma}^-$ at center-of-mass energies between 3.510 and 4.951 GeV, J. High Energy Phys. 05 (2024) 22; Measurements of Σ electromagnetic form factors in the time-like region using the untagged initial-state radiation technique, Phys. Rev. D **109**, 034029 (2024).

[47] M. Ablikim *et al.* (BESIII Collaboration), Measurement of the cross section for $e^+e^- \to \Xi^-\bar{\Xi}^+$ and observation of an excited Ξ baryon, Phys. Rev. Lett. **124**, 032002 (2020); Measurement of the cross section of $e^+e^- \to \Xi^-\bar{\Xi}^+$ at center-of-mass energies between 3.510 and 4.843 GeV, J. High Energy Phys. 11 (2023) 228.